A Multi-Functional Fully Distributed Control Framework for AC Microgrids

Shafiee, Qobad; Nasirian, Vahidreza ; Quintero, Juan Carlos Vasquez; Guerrero, Josep M.; Davoudi, Ali

Published in:
I E E E Transactions on Smart Grid

DOI (link to publication from Publisher):
10.1109/TSG.2016.2628785

Publication date:
2018

Document Version
Early version, also known as pre-print

A Multi-Functional Fully Distributed Control Framework for AC Microgrids

Qobad Shafiee, *Member, IEEE*, Vahidreza Nasirian, *Student Member, IEEE,* Juan C. Vasquez, Senior *Member, IEEE,* Josep M. Guerrero*, Fellow, IEEE,* and Ali Davoudi, *Senior Member, IEEE.*

Abstract—This paper proposes a fully distributed control methodology for secondary control of AC microgrids. The control framework includes three modules: voltage regulator, reactive power regulator, and active power/frequency regulator. The voltage regulator module maintains the average voltage of the microgrid distribution line at the rated value. The reactive power regulator compares the local normalized reactive power of an inverter with its neighbors' powers on a communication graph and, accordingly, fine-tunes Q-V droop coefficients to mitigate any reactive power mismatch. Collectively, these two modules account for the effect of the distribution line impedance on the reactive power flow. The third module regulates all inverter frequencies at the nominal value while sharing the active power demand among them. Unlike most conventional methods, this controller does not utilize any explicit frequency measurement. The proposed controller is fully distributed; i.e., each controller requires information exchange with only its neighbors linked directly on the communication graph. Steady-state performance analysis assures the global voltage regulation, frequency synchronization, and proportional active/reactive power sharing. An AC microgrid is prototyped to experimentally validate the proposed control methodology against the load change, plug-and-play operation, and communication constraints such as delay, packet loss, and limited bandwidth.

***Index Terms*— AC microgrid, cooperative control, distributed control, droop control, inverters, secondary control.**

I. Introduction

Inverter-intensive AC microgrids are viable solutions for scalable integration of distributed energy resources [1]. Control objectives are usually defined and acted upon using a hierarchical structure [1]–[3]. The primary control, conventionally implemented using a droop mechanism, provides frequency and voltage regulation and shares the active/reactive load demands in proportion to the inverters' power ratings [4]. Despite operational simplicity and decentralized structure, droop control has practical limitations: operational frequency/voltage deviation, poor reactive power sharing in the presence of distribution line impedance, and poor power quality performance when dealing with nonlinear loads, to name a few [5], [6]. A secondary control is often used to compensate for the limitations of the droop mechanism [2].

The majority of existing secondary control solutions are structured centrally, e.g., those used for frequency and voltage restoration [7], [8], reactive power sharing [9], and voltage unbalance/harmonic compensation [10]. This structure, however, has several limitations. It requires point-to-point communication between the central controller and all inverters, which increases system complexity and compromises its scalability and reliability. The centralized controller typically needs global knowledge about the system parameters and the load. Thus, it is unable to meet the plug-and-play operational requirement of microgrid systems. It is usually costly both in communication and computation when the number of sources increases. Most importantly, the central controller exposes a single point-of-failure, i.e., any failure in the controller renders the entire system inoperable. Distributed control schemes have been recently offered as alternative solutions [11]–[17], given their scalability, sparse network, and improved resiliency to faults or unknown parameters [16].

Distributed control approaches in [18]–[28] are mostly based on consensus protocols that ensure agents converge to a consistent understanding of their shared information in a distributed manner [29]. The majority of such approaches handle frequency regulation [11], [26], [28] and/or voltage control [21], [24]. Simultaneous frequency and voltage regulation is addressed in [20], while reactive power sharing is not considered. Power sharing is an important performance criterion in microgrid operation [13], [30], e.g., to prevent overloading. [21] and [22] provide global voltage regulation with proper reactive power sharing in the presence of distribution line impedances. These works replace the conventional voltage droop control, and are considered as a droop-free control methodology. One drawback of such techniques is the absence of the droop mechanism, as a backup controller, which can degrade these controllers' functionality if the communication network fails Combining frequency/voltage regulation and load power sharing objectives in a single consensus-based framework is discussed in [18], [19], [22], [27].

This paper extends the previous work of the authors in [24], to introduce a fully distributed secondary control framework which guarantees global voltage and frequency regulation as well as accurate active/reactive power sharing in droop-based microgrids. This control framework uses only sparse communication among neighboring inverters. The proposed methodology features a plug-and-play environment; prior system knowledge is not required, and inverters can be

This work has been supported in part by the National Science Foundation under grant ECCS-1405173, and by the U.S. Office of Naval Research under N00014-14-1-0718.

Q. Shafiee is with Department of Electrical and Computer Engineering, University of Kurdistan, Sanandaj, Kurdistan, Iran (e-mail: q.shafiee@uok.ac.ir). Q. Shafiee was also on leave with the University of Texas at Arlington. J. C. Vasquez, and J. M. Guerrero are with the Institute of Energy Technology, Aalborg University, Aalborg, Denmark (e-mail: juq@et.aau.dk; joz@et.aau.dk). V. Nasirian is with the TeraDiode, Inc. He was formerly with the University of Texas at Arlington (e-mail: vahidnasirian@teradiode.com). A. Davoudi is with the Department of Electrical Engineering, University of Texas at Arlington, TX, USA (e-mail: davoudi@uta.edu).

arbitrarily added to or removed from the microgrid. The salient features of this paper are outlined below:

- Conventional controllers require frequency measurement carried from the microgrid bus centrally, while the existing distributed solutions for frequency/active power control employ either local frequency measurement (e.g., [18]–[20], [23]), or local frequency variable provided by the droop mechanism (e.g., [11], [26], [27]). Our proposed method, alternatively, uses active power measurements to successfully synchronize frequencies across the microgrid without the need for additional apparatuses for frequency measurement. This approach liberates the controller from frequency measurement loops.
- In practical distribution network with non-negligible impedances, there exists a conflict between voltage regulation and accurate reactive power sharing. The existing voltage/reactive power controllers provide either precise voltage regulation (e.g., [18]–[20]) or a tunable compromise between voltage regulation and reactive power sharing (e.g., [27]). The former approach does not achieve reactive power sharing, while the later leads to a poor voltage regulation. Alternatively, the proposed controller guarantees successful global voltage regulation with accurate reactive power sharing. Unlike [21], the proposed reactive power controller shares the power via fine-tuning the Q-V droop coefficients; each source participates in reactive power support according to its predefined power rating.
- The proposed method can relapse to droop mechanism if the overall communication system fails. Similar distributed solutions (e.g., in [21], [22]) do not accommodate such contingency, and are vulnerable to communication failure.
- The controller objectives, i.e., managing voltage, frequency, and load sharing, are analytically shown to be met in the steady state. The controller performance is then evaluated on an experimental AC microgrid prototype.

The remainder of this paper is organized as follows: The proposed cooperative control framework is introduced in Section II. Steady-state analysis for the microgrid operating with the proposed controller is provided in Section III. Section IV experimentally validates the proposed controller for an AC microgrid prototype. Section V concludes the paper.

II. Distributed Control Framework

Figure 1 depicts the general structure of an inverter-interfaced microgrid control architecture augmented with a distributed secondary control. It has three control modules (see Fig. 3): voltage regulator, reactive power regulator, and active power/ frequency regulator. The voltage regulator module adjusts the global voltage across the distribution bus at the rated value. The reactive power regulator tunes the droop coefficients to provide proportional reactive power sharing, i.e., the total inductive load is shared among sources in proportion to their rated reactive powers. The third control module regulates the microgrid's frequency while maintaining the proportional active power sharing feature of the droop mechanism. The active and reactive power sharing are achieved within the predefined (active/reactive) power ratings of microgrid sources.

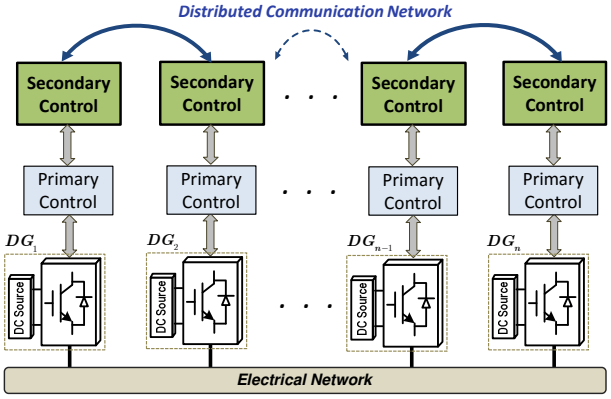

Fig. 1. Microgrid control architecture with a distributed secondary control.

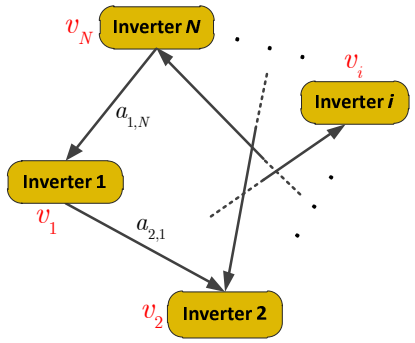

Fig. 2. Graphical representation of information exchange among inverters.

As shown in Fig. 3, the proposed controller's outputs ($\delta\omega_i, \delta e_i, \delta n_i$) at each inverter, e.g., inverter *i,* are added to the well-known droop control mechanism, i.e.,

$$\omega_i^* = \omega^{\text{rated}} - m_i p_i \tag{1}$$

$$e_i^* = e^{\text{rated}} - n_i q_i \tag{2}$$

to update the set points of the line-to-neutral voltage magnitude, e_i^*, and frequency, ω_i^*. Accordingly, a suitable three-phase voltage reference, v_i^*,

$$v_i^*(t) = e_i^*(t)\sin\left(\int_0^t \omega_i^*(\tau)d\tau\right), \tag{3}$$

is generated as a reference for the voltage and current control loops. While the voltage controller produces current reference, the current controller regulates the output current to follow that reference. Accordingly, the space-vector PWM module assigns appropriate switching signals to drive the inverter. The current control loop is normally set to be five times faster than the voltage loop with their bandwidth in the order of a few kHz (e.g., 2 kHz). Bandwidths of the upper control loops varies from a few to tens of Hz (e.g., 100 Hz for the droop control and 10 Hz for the secondary control). More details and guidelines for an optimal design of current/voltage control loops and droop control can be found in [30].

The microgrid system, as illustrated in Figs. 1 and 3, is composed of three layers: electrical (physical) layer, control layer, and cyber (communication network) layer. The electrical layer includes the power distribution network and

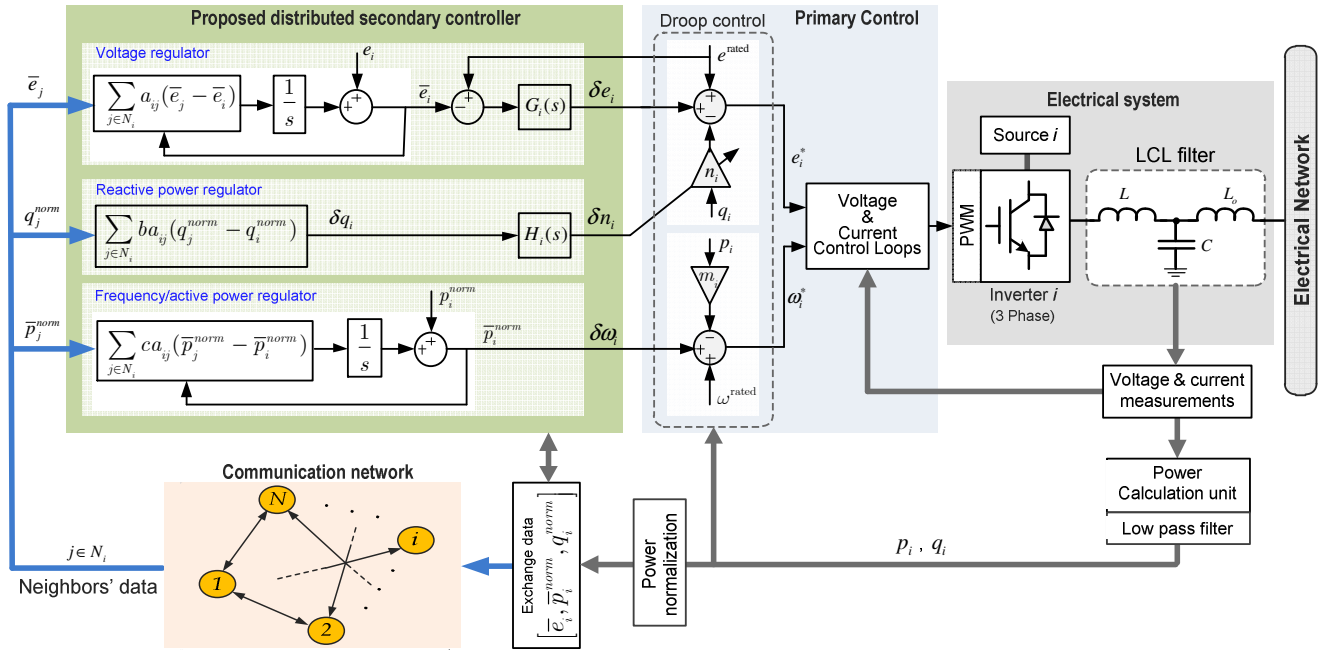

Fig. 3. Proposed distributed control framework for the *i*-th inverter.

power electronics interfacing. Such a physical system can be equipped with a cyber network to exploit different control paradigms. The control layer includes the distributed control modules along with the primary control loop, and can be coupled with the physical network via sensors and controllers embedded in power electronics devices. The cyber layer facilitates data exchange among different power electronics inverters to collectively achieve consensus on qualities of interest. The cyber communication layer can be actualized and interfaced with the control layer using different communication protocols, for example, wireless Zigbee. A brief review on graph theory and preliminary requirements for the proposed controller is presented in the following subsection.

A. *Communication Network Requirements*

With a proper design of the communication graph, the control variables (on all nodes) reach a global consensus. It should be noted that the communication network can have a different topology than the underlying microgrid. The communication network may form a weighted graph among inverters, as shown in Fig. 2. The graph is represented as a set of nodes $\mathbf{V}=\{v_1,v_2,...,v_N\}$ connected through a set of edges $\mathbf{E}\subset\mathbf{V}\times\mathbf{V}$ with an associated adjacency matrix $\mathbf{A}=[a_{ij}]\in\mathrm{R}^{N\times N}$, where N is the number of nodes (i.e., inverters). A direct path from v_i to v_j is a sequence of edges that connects the two nodes. The Adjacency matrix $\mathbf{A}$ carries the communication weights, where $a_{ij}>0$ if $(v_j,v_i)\in\mathbf{E}$, i.e., node i receives data from node j, and $a_{ij}=0$ otherwise. For the purpose of this paper, we assume a fixed adjacency matrix. $N_i=\{j\,|\,(v_j,v_i)\in\mathbf{E}\}$ denotes the set of all neighbors of the corresponding node i. Equivalently, if $j\in N_i$, then v_i receives information from v_j. However, in a directed graph, the links are not necessarily reciprocal, i.e., v_j may not receive information from v_i. If there exists at least a direct path to every other node, the eventual convergence of the control variables to the desired reference set points, i.e., the consensus, is guaranteed [29].

The controller at node i, relays an information vector, Ψ_i, to its neighbors on the communication graph. The information vector includes the estimate of the averaged voltage magnitudes, $\overline{e}_i$, the estimate of the averaged normalized active powers, $\overline{p}_i^{\mathrm{norm}}$, and the normalized reactive powers, q_i^{norm}, at node i. The term *normalized* refers to the supplied active/ reactive power by the inverter *i* multiplied by its corresponding droop coefficient, i.e., $p_i^{\mathrm{norm}}=m_{i0}p_i$ and $q_i^{\mathrm{norm}}=n_{i0}q_i$. Droop coefficients are conventionally defined according to an acceptable range of voltage/frequency deviations from the rated voltage/frequency divided by the inverters' rated active/reactive powers, e.g., $n_{i0}=\Delta e/q_i^{rated}$ and $m_{i0}=\Delta\omega/p_i^{rated}$, for inverter *i*. The term *magnitude* indicates the peak value of the voltage waveform measured in volts.

It should be noted that the proposed methodology requires a sparse communication network, undirected or directed, that carries, at least, a root node with a direct path to every other node, and a balanced Laplacian matrix. As long as these requirements are met, there is no limitation on the number of sources/inverters; they can be arbitrarily added to or removed from the microgrid.

B. *Voltage Regulator Module*

The proposed voltage regulator is inspired by the power-flow analysis of large-scale power systems. Therein, not all bus voltages are 1 pu; rather, the dispatch center assigns values close to the rated voltage (e.g.,

$0.95\ pu \le e_i^* \le 1.05\ pu$) to enable a desired power flow. The voltage regulator provides a voltage correction term, δe_i, to boost the voltage magnitude at the terminals of inverter i. Each controller has an estimator, highlighted in Fig. 3, that estimates the average of the voltage magnitudes across the distribution line, $\overline{e}_i$.

The estimator module at node i provides the estimation of the average voltage magnitude, $\overline{e}_i$, and exchanges this estimation with its neighbors. This estimation is based on the so-called dynamic consensus protocol [31]

$$\overline{e}_i(t) = e_i(t) + \int_0^t \sum_{j\in N_i} a_{ij}\left(\overline{e}_j(\tau) - \overline{e}_i(\tau)\right)d\tau, \tag{4}$$

where $\overline{e}_j$ is the estimate of the average voltage magnitude provided by the estimator module at node j. In the updating protocol, the local voltage, e_i, is directly fed into the estimation process which implies that any voltage variation at node i immediately affect the estimation at that node, $\overline{e}_i$. The difference between this estimation and the rated voltage magnitude, e^{rated}, is then fed to a PI controller, $G_i(s)$, to obtain the voltage correction term, δe_i.

Unlike most existing methods, where the sources share identical voltage set points in the steady state, i.e., $e_1^* = \cdots = e_N^* = e^{\text{rated}}$, our method ensures that the voltage set points are maintained within an acceptable range of the rated voltage. Uneven voltage set points offer the opportunity to accurately share the reactive power, while accounting for the distribution line impedances.

C. Reactive Power Regulator Module

Performance of $Q-V$ droop controller is compromised in the presence of the distribution line impedances. The reactive power regulator module at each inverter tunes the droop coefficients according to microgrid's loading condition. The reactive power regulator at node i receives the normalized reactive powers of all its neighbors, i.e., the terms q_j^{norm} from all nodes j, $j \in N_i$. Then, its normalized reactive power is compared with a weighted average of its neighbors' powers to find the loading mismatch, δq_i,

$$\begin{aligned}\delta q_i &= \sum_{j\in N_i} b a_{ij}(q_j^{\text{norm}} - q_i^{\text{norm}}) \\ &= \sum_{j\in N_i} b a_{ij}\left(q_j^{\text{norm}}\right) - b(\sum_{j\in N_i} a_{ij}) q_i^{\text{norm}}.\end{aligned} \tag{5}$$

b is the coupling gain between the voltage and reactive power regulators. This allows us to use the communication network of the voltage regulator module. As seen in Fig. 3, the loading mismatch, δq_i, is fed to a PI controller, $H_i(s)$, to generate the droop correction term, δn_i. This correction term is, then, used to update the droop coefficient,

$$n_i(t) = n_{i0} - \delta n_i(t). \tag{6}$$

n_{i0} is the initial droop assignment. This adjustment helps reduce the loading mismatch among neighbor inverters and, ultimately, the whole microgrid. Equivalently, the reactive powers reach consensus, and the mismatch terms converge to zero in the steady state, if the communication graph satisfies a balanced Laplacian matrix (see Section III). The adaptive behavior of Q-V droop mechanism provided by the proposed method has been illustrated by a diagonal arrow in Fig. 3.

D. Frequency Regulator Module

Conventional frequency synchronization methods utilize feedback mechanisms that require frequency measurement. This could lead to a slow frequency response and a relatively large frequency deviation in presence of disturbances. In this subsection, we propose a simple control module that does not require frequency measurement, leading to a smaller frequency deviation.

The frequency control module provides an estimated average of the normalized active power, $\overline{p}_i^{\text{norm}}$. Similar to the voltage estimation process, this estimation is made using a dynamic consensus protocol, as highlighted in Fig. 3. This average value is then used as a global signal to be added to the $P-\omega$ droop mechanism. Accordingly, the controller at node *i* updates its average value dynamically based on

$$\overline{p}_i^{norm}(t) = p_i^{norm}(t) + \int_0^t \sum_{j\in N_i} c a_{ij}\left(\overline{p}_j^{norm}(\tau) - \overline{p}_i^{norm}(\tau)\right)d\tau, \tag{7}$$

where the coupling gain *c* is a design parameter, and $\overline{p}_j^{\text{norm}}$ is the normalized average active power provided by the estimator at node j linked with node *i*. As seen in (7), the updating protocol uses the local normalized active power, p_i^{norm}, to account for the active power variation in the estimation process.

The control methodology in this work is introduced for dispatchable sources interfaced with voltage-source converters, e.g. energy storage systems. In such cases, active/reactive power rates are known and fixed, thus normalized powers can be easily obtained. In non-dispatchable sources, e.g., renewable energy sources, however, the output power is stochastic and a function of ambient conditions. In a scenario where some sources are non-dispatchable, the rated powers can be set at the maximum power supplied by that source.

E. Controller Design Guideline

Appropriate selection of control parameters is essential to the proper operation of the proposed control methodology. The proposed methodology requires a sparse communication network to exchange information. This network must feature a balanced Laplacian matrix and carry, at least, a root node with a direct path to every other node. Control modules may operate in different time frames. To be more specific:

1) Voltage observers are the most inner loops in this control framework and will be the fastest. They quickly provide voltage estimations for the voltage controller, G_i, to maintain voltage stability and regulation. Communication gains, a_{ij}s, are the building blocks of the Laplacian matrix, L, whose eigenvalues define the observer dynamics. As long as the stability and communication bandwidth is taken into account, the gains can be chosen large enough to speed up the response. The voltage controllers, G_is, should be chosen such

that the voltage control loop has a bandwidth of about ten-times less than the microgrid (open-loop) dynamics.

2) As opposed to the voltage regulation, the active/reactive power regulators respond relatively slow. The goal of these regulators is to accurately share active/reactive power in the steady state, while their transient performances are of less importance. It is also important that low-bandwidth power measurement filters (for noise attenuation) naturally slow down the dynamic response of the power sharing control loops. Accordingly, the coupling gains, b, c, must be selected to provide such desired performance for the power regulators; relatively smaller gains help stabilize the entire system.

More details for optimal design of communication weights and impact of communication constraints including delays and switching of topology on the consensus protocols can be found in [32], [33].

III. Steady-state Analysis

This section validates the controller operational requirements, i.e., global voltage regulation, frequency synchronization, and proportional power sharing in the steady state. Since the inverters' rated voltages are generally assumed to be the microgrid's rated (line-to-neutral) voltage magnitudes, e^{rated}, with no loss of generality, one can assume $\mathbf{e}^{\text{rated}} = e^{\text{rated}}\underline{\mathbf{1}}$.

Let's assume that the microgrid operates in the steady state for $t \geq t_0$. One can note that all voltage estimators converge to the true average voltage at the distribution buses, i.e.,

$$\overline{\mathbf{e}}^{\text{ss}} = \left(\frac{1}{N}\sum_{i=1}^{N} e_i^{\text{ss}}\right)\underline{\mathbf{1}} = \left\langle e^{\text{ss}}\right\rangle \underline{\mathbf{1}}, \tag{8}$$

where x^{ss} (e.g., e^{ss}) represents the steady-state value of the x (e.g., e), and $\left\langle e^{\text{ss}}\right\rangle$ represents the average value of e^{ss}. Note that the analytics here evaluates the average of the voltages, $\langle e^{\text{ss}}\rangle$, to ensure successful regulation of the average voltage at the rated value, i.e., $\left\langle e^{\text{ss}}\right\rangle = e^{\text{rated}}$.

Based on the control routine shown in Fig. 3 (i.e., equations (4), (5), and (6)), one can write the vectors of voltage correction terms, $\Delta\mathbf{e} = [\delta e_1, \delta e_2, ..., \delta e_N]^{\text{T}}$, and droop correction terms, $\Delta\mathbf{n} = [\delta n_1, \delta n_2, ..., \delta n_N]^{\text{T}}$, in the steady state, as

$$\Delta\mathbf{e}^{\text{ss}} = \mathbf{G}_{\text{P}}(\mathbf{e}^{\text{rated}} - \overline{\mathbf{e}}^{\text{ss}}) + \mathbf{G}_{\text{I}}(\mathbf{e}^{\text{rated}} - \overline{\mathbf{e}}^{\text{ss}})(t - t_0) + \mathbf{K}_{\text{e}}(t_0) \tag{9}$$

$$\Delta\mathbf{n}^{\text{ss}} = \mathbf{H}_{\text{P}}(-b\mathbf{L}\mathbf{q}^{\text{norm,ss}}) + \mathbf{H}_{\text{I}}(-b\mathbf{L}\mathbf{q}^{\text{norm,ss}})(t - t_0) + \mathbf{K}_{\text{n}}(t_0) \tag{10}$$

$\mathbf{G}_{\text{P}}$ (or, $\mathbf{H}_{\text{P}}$) and $\mathbf{G}_{\text{I}}$ (or, $\mathbf{H}_{\text{I}}$) are diagonal matrices carrying the proportional and integral gains of the voltage controller (or, the reactive power controller) matrix $\mathbf{G}$ (or, $\mathbf{H}$), and $\mathbf{K}_{\text{e}}(t_0)$ and $\mathbf{K}_{\text{n}}(t_0)$ are column vectors that carry the controllers output at $t = t_0$. The term $-b\mathbf{L}\mathbf{q}^{\text{norm,ss}}$ expresses the matrix format for the reactive power comparator of (5), in the steady state. $\mathbf{q}^{\text{norm}} = [q_1^{\text{norm}}, q_2^{\text{norm}}, ..., q_N^{\text{norm}}]^{\text{T}}$ is the column vector of normalized reactive powers, and $\mathbf{L}$ represents the Laplacian matrix.

Similarly, the vector of local voltage set points, $\mathbf{e}^* = [e_1^*, e_2^*, ..., e_N^*]^{\text{T}}$, in the steady state, can be written as

$$\mathbf{e}^{*\text{ss}} = \mathbf{e}^{\text{rated}} + \Delta\mathbf{e}^{\text{ss}} - \text{T}(\mathbf{n}_0 - \Delta\mathbf{n}^{\text{ss}})\mathbf{q}^{\text{ss}}, \tag{11}$$

where $\mathbf{q} = [q_1, q_2, ..., q_N]^{\text{T}}$ is the column vector of supported reactive powers, and $\mathbf{n}_0$ carries column vectors of initial droop coefficients. $\text{T}(\cdot) = \text{R}^{\text{N}\times 1} \rightarrow \text{R}^{\text{N}\times\text{N}}$ is the transformation that maps a vector to a diagonal matrix,

$$\text{T}([x_1, x_2, ..., x_N]^{\text{T}}) = \text{diag}\{x_1, x_2, ..., x_N\}. \tag{12}$$

By substituting (9) and (10) in (11),

$$\begin{aligned}\mathbf{e}^{*\text{ss}} = {} & e^{\text{rated}}\underline{\mathbf{1}} \\ & + (\mathbf{G}_{\text{P}} + \mathbf{G}_{\text{I}}(t - t_0))(e^{\text{rated}} - \left\langle e^{\text{ss}}\right\rangle)\underline{\mathbf{1}} + \mathbf{K}_{\text{e}}(t_0) \\ & - \text{T}(\mathbf{n}_0 + (\mathbf{H}_{\text{P}} + \mathbf{H}_{\text{I}}(t - t_0))(b\mathbf{L}\mathbf{q}^{\text{norm,ss}}) - \mathbf{K}_{\text{n}}(t_0))\mathbf{q}^{\text{ss}}\end{aligned} \tag{13}$$

Equation (13) provides the steady-state voltage set points, $\mathbf{e}^{*\text{ss}}$, for $t \geq t_0$. In the steady state, the time-dependent part of (13) is zero, i.e.,

$$\mathbf{G}_{\text{I}}(e^{\text{rated}} - \left\langle e^{\text{ss}}\right\rangle)\underline{\mathbf{1}} - \text{T}(b\mathbf{H}_{\text{I}}\mathbf{L}\mathbf{q}^{\text{norm,ss}})\mathbf{q}^{\text{ss}} = 0. \tag{14}$$

Since $\mathbf{H}_{\text{I}}$ is a diagonal matrix and b is a real number, one can write,

$$\text{T}(b\mathbf{H}_{\text{I}}\mathbf{L}\mathbf{q}^{\text{norm,ss}}) = b\mathbf{H}_{\text{I}}\text{T}(\mathbf{L}\mathbf{q}^{\text{norm,ss}}). \tag{15}$$

This transformation helps to reorder (14) as

$$(e^{\text{rated}} - \left\langle e^{\text{ss}}\right\rangle)\mathbf{U}\underline{\mathbf{1}} = \text{T}(\mathbf{L}\mathbf{q}^{\text{norm,ss}})\mathbf{q}^{\text{ss}}, \tag{16}$$

where

$$\begin{aligned}\mathbf{U} &= b^{-1}\mathbf{G}_{\text{I}}\mathbf{H}_{\text{I}}^{-1} \\ &= \text{diag}\left\{\mathbf{G}_{\text{I}}(i,i)/b\mathbf{H}_{\text{I}}(i,i)\right\} = \text{diag}\left\{u_i\right\}\end{aligned} \tag{17}$$

is a diagonal matrix with positive entries, i.e., $u_i > 0$. Accordingly,

$$(e^{\text{rated}} - \left\langle e^{\text{ss}}\right\rangle)[u_1, u_2, ..., u_N]^{\text{T}} = \text{T}(\mathbf{L}\mathbf{q}^{\text{norm,ss}})\mathbf{q}^{\text{ss}}. \tag{18}$$

If any of the reactive powers is zero, e.g., $q_i = 0$, then (18) implies $e^{\text{rated}} = \left\langle e^{\text{ss}}\right\rangle$. Otherwise, one can safely assume that all the sources either only deliver or only receive reactive power, i.e., all $q_i > 0$ or all $q_i < 0$. The scenario in which $q_i > 0$ for some sources and $q_i < 0$ for others is not practical as it leads to unnecessary reactive power circulations among inverters. Thus, considering (13), one can simplify (18) as,

$$(e^{\text{rated}} - \left\langle e^{\text{ss}}\right\rangle)[\frac{u_1}{q_1^{\text{ss}}}, \frac{u_2}{q_2^{\text{ss}}}, ..., \frac{u_N}{q_N^{\text{ss}}}]^{\text{T}} = \mathbf{L}\mathbf{q}^{\text{norm,ss}} \tag{19}$$

Multiplying both sides of (19) from the left by $\mathbf{1}^{\text{T}}$ gives,

$$(e^{\text{rated}} - \left\langle e^{\text{ss}}\right\rangle)\underline{\mathbf{1}}^{\text{T}}[\frac{u_1}{q_1^{\text{ss}}}, \frac{u_2}{q_2^{\text{ss}}}, ..., \frac{u_N}{q_N^{\text{ss}}}]^{\text{T}} = \underline{\mathbf{1}}^{\text{T}}\mathbf{L}\mathbf{q}^{\text{norm,ss}}. \tag{20}$$

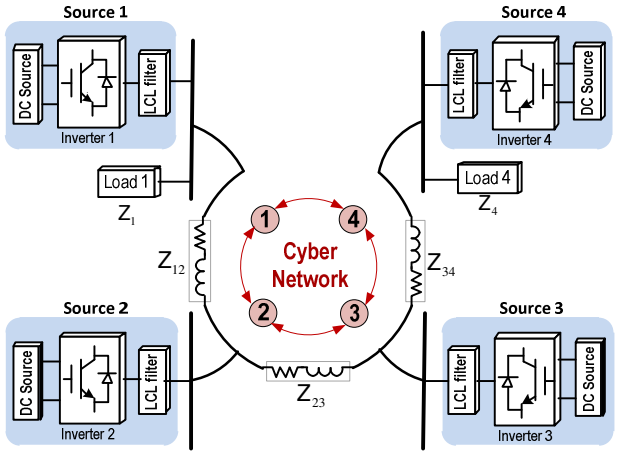

(a)

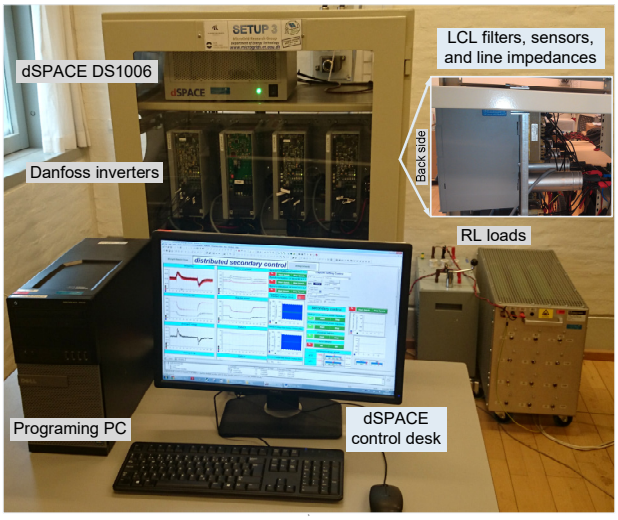

(b)

Fig. 4. The microgrid test bench: a) schematic of the microgrid including the physical system and the communication network. b) the hardware prototype.

Given the balanced Laplacian matrix, $\underline{\mathbf{1}}^{\mathrm{T}}\mathbf{L}=0$ [15],

$$(e^{\mathrm{rated}}-\left\langle e^{\mathrm{ss}}\right\rangle)\sum_{j=1}^{N}\frac{u_j}{q_j^{\mathrm{ss}}}=0\,. \tag{21}$$

Since $u_j>0$, the sigma term is nonzero and $e^{\mathrm{rated}}-\left\langle e^{\mathrm{ss}}\right\rangle=0$. Therefore, the averaged voltage magnitude, $\left\langle e^{\mathrm{ss}}\right\rangle$, is successfully regulated at the rated value, e^{rated}. By substituting $e^{\mathrm{rated}}-\left\langle e^{\mathrm{ss}}\right\rangle=0$ into (19),

$$(e^{\mathrm{rated}}-\left\langle e^{\mathrm{ss}}\right\rangle)\sum_{j=1}^{N}u_j=\mathbf{L}\mathbf{q}^{\mathrm{norm,ss}}\mathbf{q}^{\mathrm{ss}}=0\,, \tag{22}$$

which is a quadratic equation. It is shown in [15] that if the communication graph contains some minimum connectivity, the only nonzero solution to $\mathbf{L}\mathbf{x}=0$ is $\mathbf{x}=k\underline{\mathbf{1}}$, where k is a real number. Thus, (22) implies $\mathbf{q}^{\mathrm{ss}}=k(\mathbf{q}^{\mathrm{norm,ss}})^{-1}\underline{\mathbf{1}}$, and ensures the proportional reactive power sharing.

The active power/frequency regulator module adjusts the system frequency by biasing the $P-\omega$ droop characteristic and tuning the set point for the angular frequency, ω_i^*. One can find from Fig. 3,

$$\omega_i^*=\omega^{\mathrm{rated}}+\overline{p}_i^{\mathrm{norm}}-p_i^{\mathrm{norm}}\,. \tag{23}$$

TABLE I
MICROGRID ELECTRICAL AND CONTROL PARAMETERS

Electrical Parameters		
Parameter	Symbol	Value
DC voltage	V_{dc}	650 V
MG voltage magnitude	e^{rated}	325 V
MG frequency	f	50 Hz
Switching frequency	f_s	10 kHz
LCL filter capacitance	C	25 µF
LCL filter inductance	L	1.8 mH
LCL filter output inductance	L_o	1.8 mH
Line impedance 1, 2	Z_{12}	R_{12}= 0.8 Ω, L_{12}=3.6 mH
Line impedance 2, 3	Z_{23}	R_{23}= 0.4 Ω, L_{23}=1.8 mH
Line impedance 3, 4	Z_{34}	R_{34}= 0.7 Ω, L_{34}=1.2 mH
Load at Bus 1	Z_1	R_1= 43 Ω, L_1=0.3 H
Load at Bus 4	Z_4	R_4= 124 Ω, L_4=0.1 H

Control Parameters			
Parameter	Symbol	Sources 1&2	Sources 3&4
Rated active power	p^{rated}	1600 W	800 W
Rated reactive power	q^{rated}	600 VAr	300 VAr
$P-\omega$ droop coefficient	m_0	0.0008 W/rd	0.0004 W/rd
$Q-V$ droop coefficient	n_0	0.01 Var/V	0.02 Var/V
$G_i(s)$ proportional term	k_{pQ}	0.01 Var/V	0.01 Var/V
$G_i(s)$ integral term	k_{iQ}	0.25 Var/V	0.25 Var/V
$H_i(s)$ proportional term	k_{pv}	0.01	0.01
$H_i(s)$ integral term	k_{iv}	2.4	2.4

Properly tuned droop gains revise the frequency and damp all possible oscillations until the entire network settles on a common frequency and all active/reactive powers converge to a steady state. It should be noted that poorly tuned droop controllers, on the contrary, may even lead to system instability. Thus, in the steady state, one can safely assume that all sources will synchronize to the same frequency, ω^{ss}, and all estimations of the averaged normalized active powers will converge to the true average value, i.e.,

$$\overline{\mathbf{p}}^{\mathrm{norm,ss}}=(\frac{1}{N}\sum_{i=1}^{N}p_i^{\mathrm{norm,ss}})\underline{\mathbf{1}}=\left\langle p^{\mathrm{norm,ss}}\right\rangle\underline{\mathbf{1}}\,. \tag{24}$$

$\left\langle p^{\mathrm{norm,ss}}\right\rangle$ represents the average value of $p^{\mathrm{norm,ss}}$.

According to Fig. 3, for any source i at $t\geq t_0$, one can write,

$$\omega^{\mathrm{ss}}=\omega^{\mathrm{ref}}+\left\langle p^{\mathrm{norm,ss}}\right\rangle-p_i^{\mathrm{norm,ss}}\,. \tag{25}$$

Equation (35) holds true for all inverters. Thus, one can conclude that for every inverter i and j, $p_i^{\mathrm{norm,ss}}=p_j^{\mathrm{norm,ss}}$. This condition satisfies the proportional active load sharing. Moreover, as all terms $p_i^{\mathrm{norm,ss}}$ have converged to the same steady-state value, $p_i^{\mathrm{norm,ss}}=\left\langle p^{\mathrm{norm,ss}}\right\rangle$. Thus, (25) implies $\omega^{\mathrm{ss}}=\omega^{\mathrm{rated}}$, i.e., all sources have been synchronized to the rated frequency, ω^{rated}.

IV. EXPERIMENTAL VALIDATION

A four-inverter microgrid setup, shown in Fig. 4, is prototyped in the Intelligent Microgrid Laboratory at Aalborg University [34]. The rated voltage and frequency are 230 V and 50 Hz, respectively. The rated powers of inverters 1 and 2 are twice those for inverters 3 and 4 (see Table I). LCL filters are installed at the inverters' outputs to reduce the switching-induced harmonics. Low-pass filters (<2 Hz) are used in the power measurements to eliminate undesired switching and line-frequency harmonics. A ring bidirectional

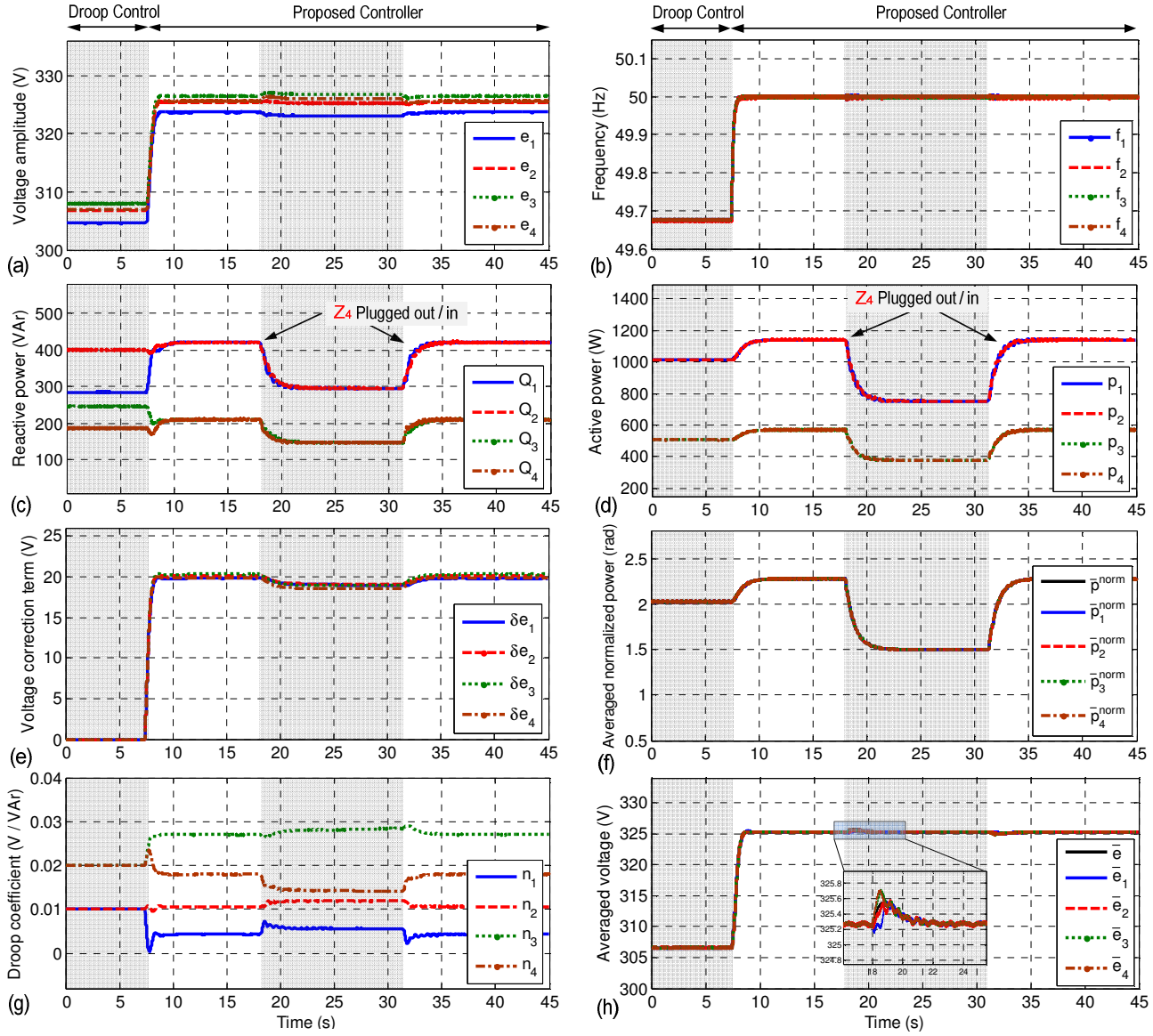

Fig. 5. Performance of the proposed controller: (a) Bus voltage magnitude, (b) Bus voltage frequency, (c) Supplied reactive power, (d) Supplied active power, (e) Voltage correction term, (f) Frequency correction term (i.e., averaged normalized powers), (g) V-Q droop coefficients, and (h) Averaged bus voltages.

communication network, highlighted in Fig. 4(a), facilitates data exchange among inverters. The communication links are all bidirectional leading to a balanced Laplacian matrix. It should be noted that alternative communication structures, with fewer links, could still meet the graphical connectivity requirement. However, an extra link is considered here to maintain the graphical connectivity even with a single link/inverter failure. A single dSPACE DS1006, as seen in Fig. 4(b), implements the control routines and mimics the distributed communication network. The proposed control framework together with the communication network model including the real constraints (i.e., delay, packet loss, and limited bandwidth) are implemented in the MATLAB/SIMULINK environment, and compiled to the dSPACE. The adjacency matrix, $\mathbf{A}$, and the coupling gains, i.e., the design parameters, b and c, are

$$\mathbf{A}=\begin{bmatrix}0 & 20 & 0 & 20\\ 20 & 0 & 20 & 0\\ 0 & 20 & 0 & 20\\ 20 & 0 & 20 & 0\end{bmatrix},\quad b=0.003,\quad c=50. \tag{26}$$

Other electrical and control parameters are tabulated in detail in Table I. Performance of the proposed cooperative controller is evaluated through the following studies.

A. *Performance Assessment*

The performance of the proposed control algorithm is compared with the conventional droop control with fixed coefficients. As shown in Fig. 5, for $t<8$ s, only the primary droop controllers are effective, and voltage and frequency terms deviate from their rated values (see Figs. 5(a), 5(b)). Moreover, the voltage across the terminals of the distribution line varies in the presence of line impedance. This undermines

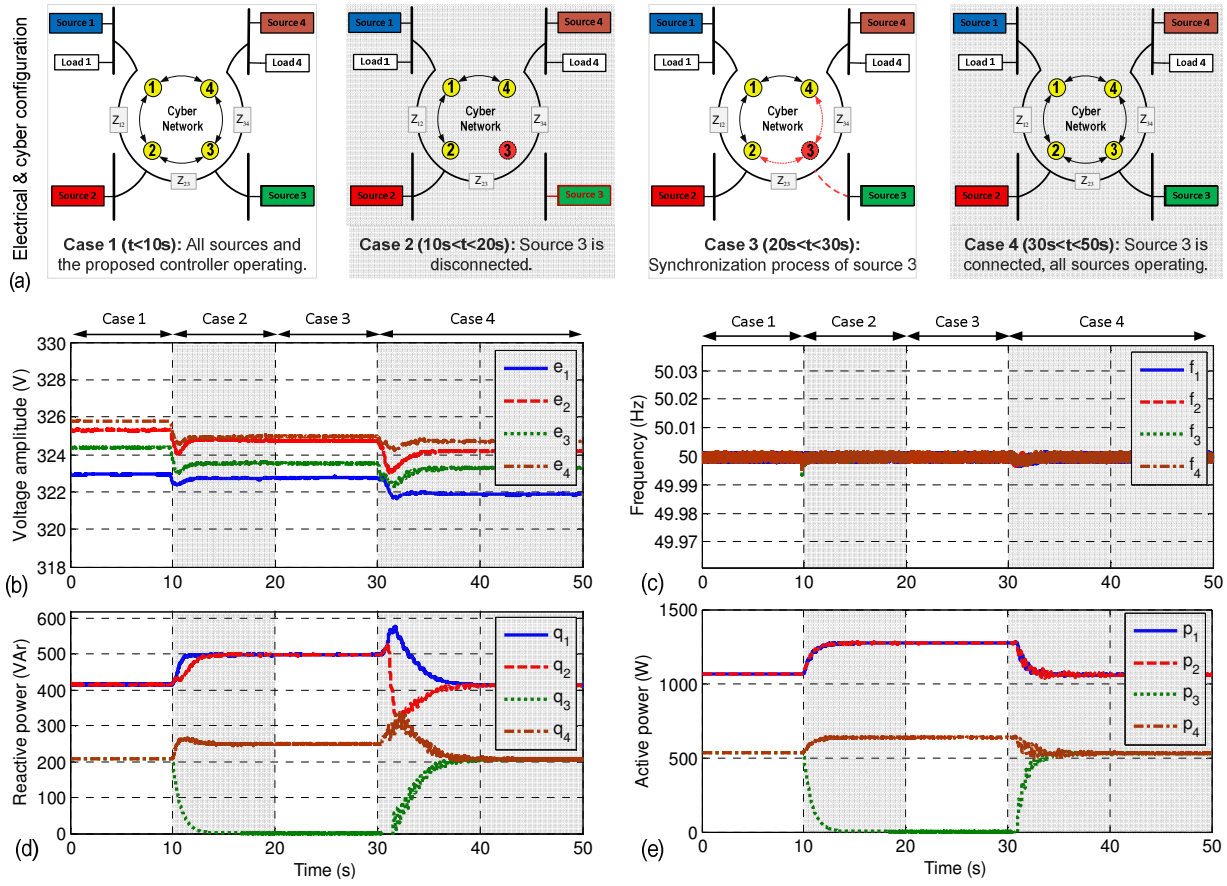

Fig. 6. Plug-and-play capability: (a) The electrical and communication network configuration, (b) Bus voltage magnitude, (c) Bus voltage frequency, (d) Supplied reactive power, and (e) Supplied active power.

the reactive power sharing process, as seen in the early part of Fig. 5(c). The active power is still proportionally shared among inverters since frequency is a global entity valid throughout the microgrid.

Once the secondary controller is activated at $t = 8$ s, the terminal voltages across the distribution line are boosted to regulate the average voltage at the rated value, (see Fig. 5(h)). Individual bus voltages ought to be different than the rated voltage to manage the reactive power flow. However, such slight deviations are kept within an acceptable range. As seen, the fine adjustment of the droop coefficient (see Fig. 5(g)) results in an accurate reactive power sharing, where the first two inverters provide twice as much reactive power as the other two inverters. Estimated average voltages are compared with the true average voltage magnitude, which is the average of the voltage terms in four inverters. An excellent agreement is reported in Fig. 5(h) between the estimations, $\overline{e}_i$s, and the true average, $\overline{e}$. The microgrid frequency is also restored to its nominal value after activating the proposed controller (see Fig. 5(b)). Estimated averages of normalized active powers, $\overline{p}_i^{\text{norm}}$ s, are compared with the true average, $\overline{p}^{\text{norm}}$, in Fig. 5(f), where an appropriate match is reported. Thus, all inverters receive the same frequency correction term, $\delta\omega_i$, to maintain the active powers sharing feature of the droop mechanism.

The local load at the fourth bus, Z_4, is unplugged at $t = 18$ s and plugged back at $t = 32$ s, to evaluate the controller performance under the load disturbances. As seen in Fig. 5, global voltage regulation, frequency regulation, and proportional active/reactive power sharing are properly carried out. Excellent voltage estimation, that tightly follows the average voltage, is reported even during transients. It should be noted that total active and reactive power demand slightly elevates after the controller activation. This effect is rooted in voltage and frequency restoration; the microgrid has to inject extra power to ensure voltage/frequency regulation at the rated values.

B. *Plug-and-Play Capability*

The controller performance for an inverter hot-swap is studied in Fig. 6. The third inverter (and its associated communication links) is intentionally disconnected from and then connected back to the microgrid (Fig. 6(a)). Removing communication links 2-3 and 3-4 still leaves a connected graph. When the third inverter is disconnected at $t = 10$ s, the voltage and frequency regulation are preserved and the excess active/reactive power demand is shared among the remaining operational inverters. It can also be seen that the active and reactive power supplied to the third bus do not suddenly drop to zero. The slow decline is because of low-pass filters placed to remove undesired harmonics from the measured power. A synchronization procedure is required to match the voltage, frequency, and phase angle of the inverter 3 with the microgrid. After successful synchronization, inverter 3 is reconnected to the microgrid at $t = 31$ s. As

Fig. 6 shows, proportional power sharing is maintained and the bus voltages/frequencies remain well regulated. The observed transient error in power sharing is because of synchronization error between inverter 3 and the microgrid at the time of connection.

C. Controller Efficacy under Directed Communication Network

Performance of the proposed control methodology under direct communication network is evaluated in Fig. 7. Fig. 7(a) displays the directed communication network in a ring structure, leading to a balanced Laplacian matrix. Only droop controllers are effective at the beginning. The proposed controller is activated at $t = 8$ s. The local load at the fourth bus is unplugged at $t = 18$ s and plugged back in at $t = 31$ s. Results show that the proposed controller has successfully maintained the global voltage regulation, frequency regulation, and proportional power sharing. Comparing Figs. 5 and 7 shows that fewer communication links does not affect the steady-state performance but only the transient response. In general, communication network configuration affects the transient response, but will not compromise the steady-state behavior, as long as the communication network remains connected and exhibits a balanced Laplacian matrix.

D. Impact of Communication Network Non-idealities

Microgrid dynamics exhibit different time scales for different levels of control hierarchy, i.e., primary, secondary, and tertiary control, as well as for different control goals (e.g., voltage regulation, frequency synchronization, etc.). In secondary control, as shown in the previous studies, the dynamics are slow and in the order of hundreds of milliseconds. Therefore, communication technologies with high data transmission rate are not required. Moreover, communication non-idealities such as delay and packet loss are expected to have a negligible impact on the controller performance. This is also shown in [7], [35]–[37], where the impact of the communication delay on load sharing and secondary frequency control has been studied. The experimental results in Figs. 8 and 9 study the effect of non-idealities in communication channels, i.e., delay, packet loss, and communication bandwidth, on the controller performance.

Figure 8 shows the controller performance in response to the step load changes under different communication delays and 98% packet loss. While sampling rates of 0.1 ms, 0.2 ms, and 1 ms, have been tested, only supplied active and reactive powers are presented for the last case, for brevity. The results show that for a relatively large amount of packet loss, and delays shorter than 400 ms, the proposed controller still remains properly functional. However, longer delays may compromise the controller performance. It should be noted that long delays and high packet loss lead to non-negligible steady-state errors in frequency and voltage terms. This is because the dynamic consensus protocol is influenced by delay and packet loss causing drift from a consensus, as shown in [38].

Further results on the impact of communication sampling rate are provided in Fig. 9. While the voltage and reactive power regulators can operate with low sampling rates, the

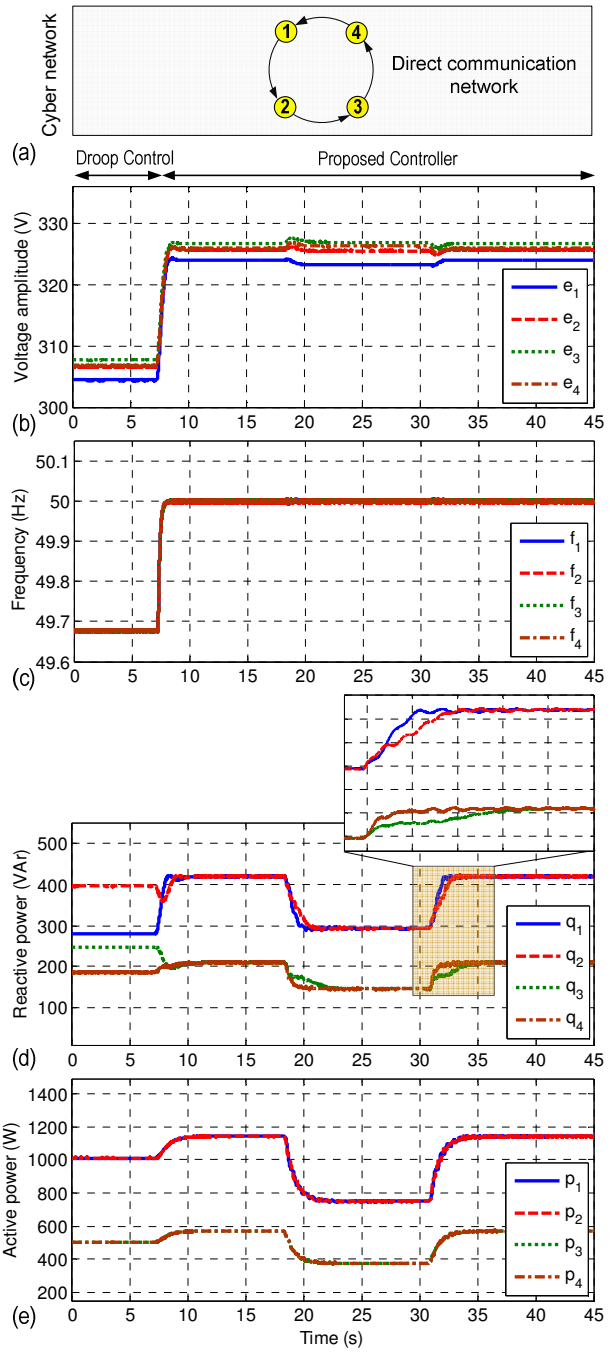

Fig. 7. Controller performance under directed cyber network: (a) The direct network used in the test system, (b) Bus voltage amplitude, (c) Bus voltage frequency, (d) Supplied reactive power, and (e) Supplied active power.

experimental studies show that the minimum operable communication rate for the frequency regulator is 1 ms. Fig. 9 demonstrates the voltage and reactive power regulator's performance when the sampling rate of communication network is 20 ms. Frequent load change occurs at bus 4 at $t = 5$ s and $t = 15$ s. To understand the relationship between the sampling rate and the other communication non-idealities, results have been provided under delay and packet loss. Comparing Fig. 9(a) and Fig. 8(b), one can conclude that sampling rate and delay are two independent issues; communication delay has almost the same impact on the controller performance for different sampling rates.

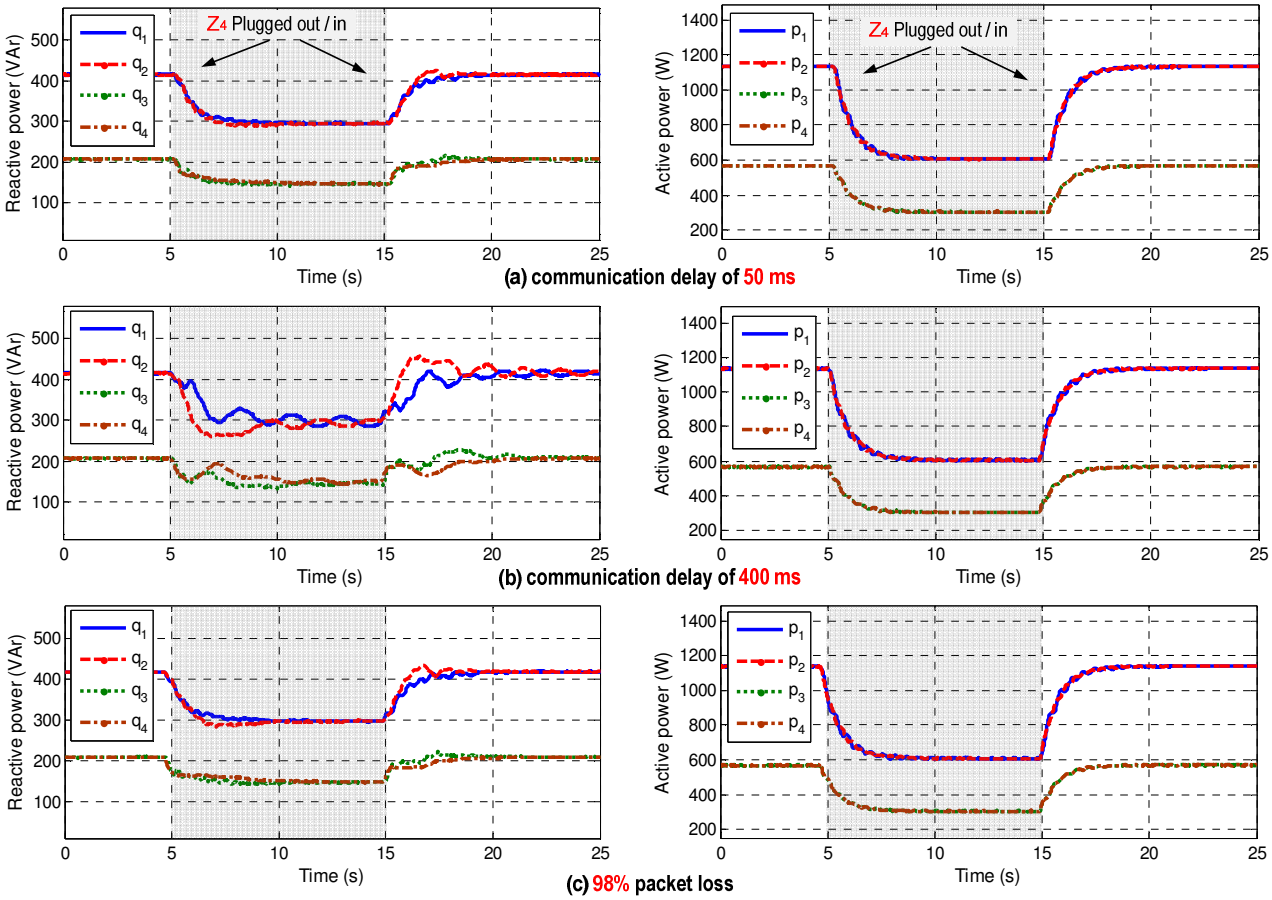

Fig. 8. Controller performance in the presence of communication non-idealities: supplied active and reactive power for (a) Delay of 50 ms, (b) Delay of 400 ms, (d) 98% packet loss.

Obviously, the lower the sampling rate, the more pronounced are the effects of packet losses on the controller performance. However, Fig. 9(b) shows that the proposed scheme is still robust against a high probability of packet loss. These observations find wireless communication technologies, e.g., 2.45 GHz ZigBee with complete data transmission delay less than 1 ms, suitable options for the field installation in a small geographical area.

V. Conclusion

A secondary control framework is introduced to handle voltage/frequency regulation and active/reactive power sharing in inverter-based microgrids. The proposed methodology is fully distributed; each inverter broadcasts an information vector only to those neighbor inverters directly linked on a communication graph. The controller of each inverter processes the local and neighbors' information using three control modules: the voltage regulator, the reactive power regulator, and the active power/frequency regulator modules. The voltage regulator module adjusts the global average voltage across the distribution bus of the microgrid, rather than the individual inverter terminal voltages, at the rated value. This enables proper sharing of the reactive power demand among inverters. The reactive power regulator module dynamically tunes the droop characteristic of each inverter by comparing the local and neighbors' reactive powers normalized with respect to their ratings. The active power/frequency regulator module estimates the average normalized active power using a dynamic consensus protocol and, accordingly, regulates the microgrid's frequency and shares the active power demand proportional to inverters' rating. The proposed control methodology accounts for the distribution line impedances, and does not require explicit measurement of the microgrid's frequency. Comparative experimental studies validate accurate global voltage regulation, frequency regulation, and proportional power sharing. Plug-and-play capability, and resiliency to different communication topologies and constraints such as limited bandwidth, delay, and packet loss, are verified through experiments.

References

[1] D. E. Olivares, A. Mehrizi-Sani, A. H. Etemadi, C. a. Cañizares, R. Iravani, M. Kazerani, A. H. Hajimiragha, O. Gomis-Bellmunt, M. Saeedifard, R. Palma-Behnke, G. a. Jiménez-Estévez, and N. D. Hatziargyriou, "Trends in microgrid control," *IEEE Trans. Smart Grid*, vol. 5, no. 4, pp. 1905–1919, July 2014.

[2] J. M. Guerrero, M. Chandorkar, T. Lee, and P. C. Loh, "Advanced Control Architectures for Intelligent Microgrids—Part I: Decentralized and Hierarchical Control," *Ind. Electron. IEEE Trans.*, vol. 60, no. 4, pp. 1254–1262, April 2013.

[3] A. Bidram and A. Davoudi, "Hierarchical structure of microgrids control system," *IEEE Trans. Smart Grid*, vol. 3, no. 4, pp. 1963–1976, Dec. 2012.

[4] J. M. Guerrero, J. C. Vásquez, J. Matas, M. Castilla, and L. García de Vicuna, "Control strategy for flexible microgrid based on parallel line-

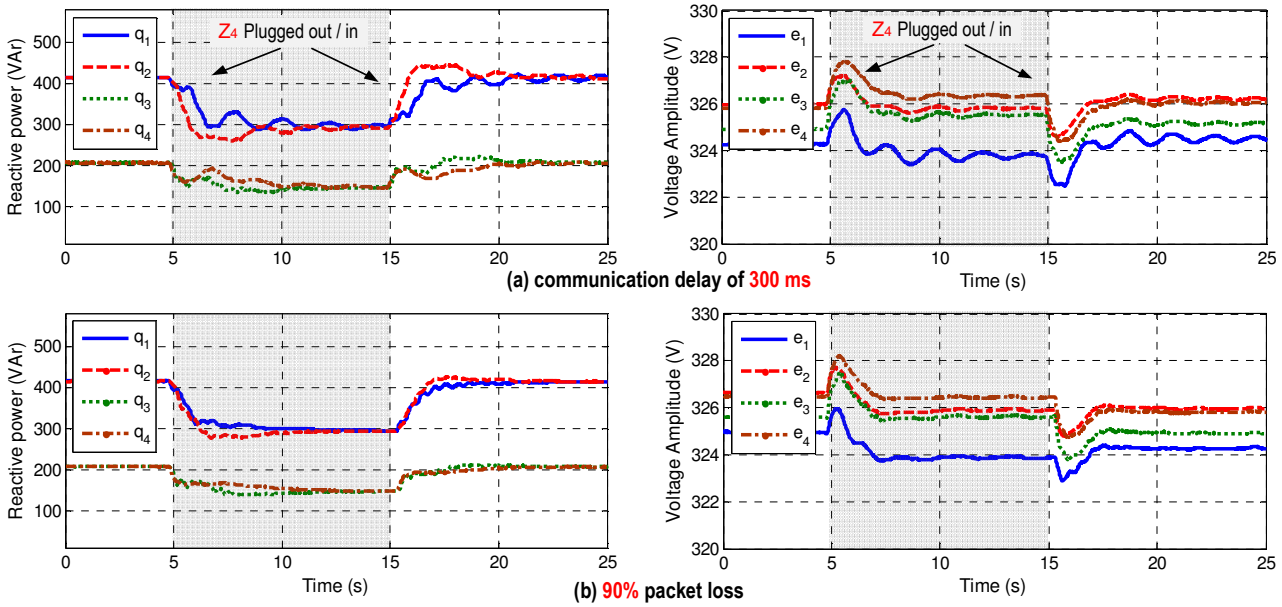

Fig. 9. Impact of communication sampling rate on the controller performance considering delay and packet loss: Supplied reactive and voltage magnitude for (a) delay of 200 ms, (b) 90% packet loss. Sampling rate of 20 ms has been examined in this case.

interactive UPS systems," *IEEE Trans. Ind. Electron.*, vol. 56, no. 3, pp. 726–736, March 2009.

[5] Q. C. Zhong, "Robust droop controller for accurate proportional load sharing among inverters operated in parallel," *IEEE Trans. Ind. Electron.*, vol. 60, no. 4, pp. 1281–1290, April 2013.

[6] J. Hu, J. Zhu, D. G. Dorrell, and J. M. Guerrero, "Virtual flux droop method - A new control strategy of inverters in microgrids," *IEEE Trans. Power Electron.*, vol. 29, no. 9, pp. 4704–4711, Sept. 2014.

[7] S. Liu, X. Wang, S. Member, P. X. Liu, and S. Member, "Impact of Communication Delays on Secondary Frequency Control in an Islanded Microgrid," *IEEE Trans. Ind. Electron.*, vol. 62, no. 4, pp. 2021–2031, April 2015.

[8] A. Mehrizi-sani and R. Iravani, "Potential-function based control of a Microgrid in islanded and grid-connected models," *IEEE Trans. Power Syst.*, vol. 25, no. 4, pp. 1883–1891, Nov. 2010.

[9] A. Micallef, M. Apap, C. Spiteri-Staines, J. M. Guerrero, and J. C. Vasquez, "Reactive power sharing and voltage harmonic distortion compensation of droop controlled single phase islanded microgrids," *IEEE Trans. Smart Grid*, vol. 5, no. 3, pp. 1149–1158, May 2014.

[10] M. Savaghebi, A. Jalilian, J. C. Vasquez, and J. M. Guerrero, "Secondary Control for Voltage Quality Enhancement in Microgrids," *IEEE Trans. Smart Grid*, vol. 3, no. 4, pp. 1893–1902, Dec. 2012.

[11] F. Dorfler, J. Simpson-Porco, and F. Bullo, "Breaking the Hierarchy: Distributed Control & Economic Optimality in Microgrids," *IEEE Trans. Control Netw. Syst.*, DOI: 10.1109/TCNS.2015.2459391, 2015.

[12] F. Guo, C. Wen, J. Mao, J. Chen, and Y.-D. Song, "Distributed Cooperative Secondary Control for Voltage Unbalance Compensation in an Islanded Microgrid," *IEEE Trans. Ind. Informatics*, vol. 11, no. 5, pp. 1078–1088, Oct. 2015.

[13] M. a Mahmud, M. J. Hossain, S. Member, H. R. Pota, and N. K. Roy, "Nonlinear Distributed Controller Design for Maintaining Power Balance in Islanded Microgrids," *IEEE Trans. ENERGY Convers.*, vol. 29, no. 4, pp. 893–903, Dec. 2014.

[14] L. Meng, X. Zhao, F. Tang, M. Savaghebi, T. Dragicevic, J. Vasquez, and J. Guerrero, "Distributed Voltage Unbalance Compensation in Islanded Microgrids by Using Dynamic-Consensus-Algorithm," *IEEE Trans. Power Electron.*, vol. 31, no. 1, pp. 827–838, Jan. 2016.

[15] V. Nasirian, S. Moayedi, A. Davoudi, and F. Lewis, "Distributed Cooperative Control of DC Microgrids," *IEEE Trans. Power Electron.*, vol. 30, no. 4, pp. 2288–2303, April 2015.

[16] M. Yazdanian, G. S. Member, and A. Mehrizi-sani, "Distributed Control Techniques in Microgrids," *IEEE Trans. Smart Grid*, vol. 5, no. 6, pp. 2901–2909, Nov. 2014.

[17] T. Morstyn, B. Hredzak, G. Demetriades, and V. Agelidis, "Unified Distributed Control for DC Microgrid Operating Modes," *IEEE Trans. Power Syst.*, vol. 31, no. 1, pp. 802–812, Jan. 2016.

[18] A. Bidram, A. Davoudi, and F. L. Lewis, "A Multiobjective Distributed Control Framework for Islanded AC Microgrids," *IEEE Trans. Ind. Informatics*, vol. 10, no. 3, pp. 1785–1798, Aug. 2014.

[19] A. Bidram, A. Davoudi, F. L. Lewis, and J. M. Guerrero, "Distributed cooperative secondary control of microgrids using feedback linearization," *IEEE Trans. Power Syst.*, vol. 28, no. 3, pp. 3462–3470, Aug. 2013.

[20] F. Guo, C. Wen, J. Mao, and Y.-D. Song, "Distributed Secondary Voltage and Frequency Restoration Control of Droop-Controlled," *IEEE Trans. Ind. Electron.*, vol. 62, no. 7, pp. 4355–4364, July 2015.

[21] J. Schiffer, T. Seel, J. Raisch, and T. Sezi, "Voltage Stability and Reactive Power Sharing in Inverter-Based Microgrids With Consensus-Based Distributed Voltage Control," *IEEE Trans. Control Syst. Technol.*, vol. 24, no. 1, pp. 96–109, Jan. 2016.

[22] V. Nasirian, Q. Shafiee, J. Guerrero, F. Lewis, and A. Davoudi, "Droop-free Distributed Control for AC Microgrids," *IEEE Trans. Power Electron.*, vol. 31, no. 2, pp. 1600–161, Feb. 2016.

[23] Q. Shafiee, J. M. Guerrero, and J. C. Vasquez, "Distributed secondary control for islanded microgrids—a novel approach," *IEEE Trans. Power Electron.*, vol. 29, no. 2, pp. 1018–1031, Feb. 2014.

[24] Q. Shafiee, V. Nasirian, J. M. Guerrero, F. L. Lewis, and A. Davoudi, "Team-oriented Adaptive Droop Control for Autonomous AC Microgrids," *IProceedings - 40th Annu. Conf. IEEE Ind. Electron. Soc. IECON*, 2014, pp. 1861 – 1867.

[25] Q. Shafiee, C. Stefanovic, T. Dragicevic, P. Popovski, J. C. Vasquez, and J. M. Guerrero, "Robust networked control scheme for distributed secondary control of islanded microgrids," *IEEE Trans. Ind. Electron.*, vol. 61, no. 10, pp. 5363–5374, Oct. 2014.

[26] J. W. Simpson-Porco, F. Dörfler, and F. Bullo, "Synchronization and power sharing for droop-controlled inverters in islanded microgrids," *Automatica*, vol. 49, no. 9, pp. 2603–2611, Sept. 2013.

[27] J. Simpson-Porco, Q. Shafiee, F. Dorfler, J. C. Vasquez, J. Guerrero, and F. Bullo, "Secondary Frequency and Voltage Control of Islanded Microgrids via Distributed Averaging," *IEEE Trans. Ind. Electron.*, vol. 62, no. 11, pp. 7025–7038, Nov. 2015.

[28] J. W. Simpson-Porco, F. Dörfler, F. Bullo, Q. Shafiee, and J. M. Guerrero, "Stability, power sharing, & distributed secondary control in droop-controlled microgrids," in *Proc. IEEE Smart Grid Commun. Symp.*, 2013, pp. 672–677.

[29] R. Olfati-Saber, J. A. Fax, and R. M. Murray, "Consensus and cooperation in networked multi-agent systems," *Proc. IEEE*, vol. 95, no. 1, pp. 215–233, Jan. 2007.

[30] J. Rocabert, A. Luna, F. Blaabjerg, and I. Paper, "Control of Power Converters in AC Microgrids," *IEEE Trans. Power Electron.*, vol. 27, no. 11, pp. 4734–4749, Nov. 2012.

[31] D. P. Spanos, R. Olfati-saber, and R. M. Murray, "Dynamic consensus for mobile network," *Proc. - 16th Int. Fed. Aut. Control*, 2005, pp. 1–6.

[32] H. Zhang, F. L. Lewis, and Z. Qu, "Lyapunov, adaptive, and optimal

design techniques for cooperative systems on directed communication graphs," *IEEE Trans. Ind. Electron.*, vol. 59, no. 7, pp. 3026–3041, July 2012.
[33] F. Xiao and L. Wang, "Asynchronous Consensus in Continuous-Time Multi-Agent Systems With Switching Topology and Time-Varying Delays," *IEEE Trans. Automat. Contr.*, vol. 53, no. 8, pp. 1804–1816, Sept. 2008.
[34] "Microgrid Research Programme," *URL: www.microgrids.et.aau.dk*.
[35] D. Rua, J. A. . Lopes, and J. Ruela, "Communications Uncertainties in Isolated Multi-Microgrid Control Systems," *Proc. Power Syst. Comput. Conf.*, 2014, pp. 1–7.
[36] C. Song, Q. Junjie, W. Dalei, and A. Keyhani, "Impact of wireless communication delay on load sharing among distributed generation systems through smart microgrids," vol. 19, no. 3, pp. 24–29, June 2012.
[37] C. Ahumada, R. Cárdenas, D. Sáez, and J. M. Guerrero, "Secondary Control Strategies for Frequency Restoration in Islanded Microgrids With Consideration of Communication Delays," *IEEE Trans. Smart Grid*, vol. 7, no. 3, pp. 1430–1441, May 2016.
[38] H. Behjati, A. Davoudi, and F. Lewis, "Modular DC–DC Converters on Graphs: Cooperative Control," *IEEE Trans. Power Electron.*, vol. 29, no. 12, pp. 6725–6741, Dec. 2014.

Qobad Shafiee (S'13-M'15) received his Ph.D. in Electrical Engineering from the Department of Energy Technology, Aalborg University, Aalborg, Denmark, in 2014. He is currently an Assistant Professor in the Department of Electrical and Computer Engineering, University of Kurdistan, Sanandaj, Iran, where he worked as a lecturer from 2007 to 2011. From March 2014 to June 2014, he was a visiting scholar at the Electrical Engineering Department, University of Texas-Arlington, Arlington, TX, USA. He worked as a postdoctoral fellow with the Department of Energy Technology, Aalborg University, in 2015. His main research interests include modeling, energy management, and control of Microgrids, modeling and control of power electronics converters. Dr. Shafiee has been Guest Associate Editor of the IEEE Journal of Emerging and Selected Topics in Power Electronics Special Issue on Structured DC Microgrids. He is currently a member of PELS, IAS, and PES Societies.

Vahidreza Nasirian is joined TeraDiode, Inc. in 2016 as High-power Electrical Engineer, where he is currently appointed as the Product Manager for high-power laser diode drivers. He received Ph.D. from the University of Texas at Arlington in 2015. His research interests include the modeling and control of power electronics, control development for microgrids, renewable/ sustainable energy systems, transportation electrification, and control of multi-agent dynamic systems. Dr. Nasirian received IEEE Power and Energy Society Prize Paper Award in Jul. 2016, Best Paper Award from IEEE Transactions on Energy Conversion in Dec. 2015, and Best Symposium Paper Award from 8th Int'l Symposium on Resilient Control Systems in Aug. 2015. He was the recipient of the UT-Arlington Graduate Dissertation Fellowship for summer 2015, the Carrizo Oil and Gas Inc. Graduate Research Fellowship for 2011–2013, and Iranian National Elites Foundation Fellowship for 2008–2010.

Juan C. Vasquez (M'12-SM'14) received the B.S. degree in electronics engineering from the Autonomous University of Manizales, Manizales, Colombia, and the Ph.D. degree in automatic control, robotics, and computer vision from the Technical University of Catalonia, Barcelona, Spain, in 2004 and 2009, respectively. He was with the Autonomous University of Manizales working as a teaching assistant and the Technical University of Catalonia as a Post-Doctoral Assistant in 2005 and 2008 respectively. In 2011, he was Assistant Professor and from 2014 he is working as an Associate Professor at the Department of Energy Technology, Aalborg University, Denmark where he is the Vice Programme Leader of the Microgrids Research Program (see microgrids.et.aau.dk). From Feb. 2015 to April. 2015 he was a Visiting Scholar at the Center of Power Electronics Systems (CPES) at Virginia Tech and a visiting professor at Ritsumeikan University, Japan. His current research interests include operation, advanced hierarchical and cooperative control, optimization and energy management applied to distributed generation in AC/DC Microgrids, maritime microgrids, advanced metering infrastructures and the integration of Internet of Things and Cyber-Physical Systems into the SmartGrid. He has authored and co-authored more than 100 technical papers only in Microgrids in international IEEE conferences and journals.

Dr. Vasquez is currently a member of the IEC System Evaluation Group SEG4 on LVDC Distribution and Safety for use in Developed and Developing Economies, the Renewable Energy Systems Technical Committee TC-RES in IEEE Industrial Electronics, PELS, IAS, and PES Societies.

Josep M. Guerrero (S'01-M'04-SM'08-FM'15) received the B.S. degree in telecommunications engineering, the M.S. degree in electronics engineering, and the Ph.D. degree in power electronics from the Technical University of Catalonia, Barcelona, in 1997, 2000 and 2003, respectively. Since 2011, he has been a Full Professor with the Department of Energy Technology, Aalborg University, Denmark, where he is responsible for the Microgrid Research Program. From 2012 he is a guest Professor at the Chinese Academy of Science and the Nanjing University of Aeronautics and Astronautics; and from 2014 he is chair Professor in Shandong University.

His research interests is oriented to different microgrid aspects, including power electronics, distributed energy-storage systems, hierarchical and cooperative control, energy management systems, and optimization of microgrids and islanded minigrids. Prof. Guerrero is an Associate Editor for the IEEE TRANSACTIONS ON POWER ELECTRONICS, the IEEE TRANSACTIONS ON INDUSTRIAL ELECTRONICS, and the IEEE Industrial Electronics Magazine, and an Editor for the IEEE TRANSACTIONS on SMART GRID and IEEE TRANSACTIONS on ENERGY CONVERSION. He has been Guest Editor of the IEEE TRANSACTIONS ON POWER ELECTRONICS Special Issues: Power Electronics for Wind Energy Conversion and Power Electronics for Microgrids; the IEEE TRANSACTIONS ON INDUSTRIAL ELECTRONICS Special Sections: Uninterruptible Power Supplies systems, Renewable Energy Systems, Distributed Generation and Microgrids, and Industrial Applications and Implementation Issues of the Kalman Filter; and the IEEE TRANSACTIONS on SMART GRID Special Issue on Smart DC Distribution Systems. He was the chair of the Renewable Energy Systems Technical Committee of the IEEE Industrial Electronics Society. In 2014 he was awarded by Thomson Reuters as Highly Cited Researcher, and in the same year he was elevated as IEEE Fellow for his contributions on "distributed power systems and microgrids."

Ali Davoudi (S'04–M'11- SM'15) received his Ph.D. in Electrical and Computer Engineering from the University of Illinois, Urbana-Champaign, IL, USA, in 2010. He is currently an Associate Professor in the Electrical Engineering Department, University of Texas, Arlington, TX, USA. He was with Solar Bridge Technologies, Champaign, IL; Texas Instruments Inc., Rochester, MN; and Royal Philips Electronics Rosemont, IL. His research interests include various aspects of analysis and control of complex power electronics systems. Dr. Davoudi is an Associate Editor for the IEEE Transactions on Transportation Electrification, IEEE Transactions on Energy Conversion, and IEEE Power Letters. He has received 2014 Ralph H. Lee Prize Paper Award from IEEE Transactions on Industry Applications, Best Paper Award from 2015 IEEE International Symposium on Resilient Control Systems, 2014-2015 Best Paper Award from IEEE Transactions on Energy Conversion, and 2016 Prize Paper Award from the IEEE Power and Energy Society.